Article

Effects of Different Admixtures on the Mechanical and Thermal Insulation Properties of Desulfurization Gypsum-Based Composites

Gengyin Cui [1,2], Dewen Kong [1,2,*] , Yingying Huang [1,2], Wei Qiu [1,2], Lili Cheng [3] and Lingling Wang [1,2]

1 College of Civil Engineering, Guizhou University, Guiyang 550025, China
2 Guizhou Provincial Key Laboratory of Rock and Soil Mechanics and Engineering Safety, Guiyang 550025, China
3 Department of Civil Engineering, Guiyang College of Information Science and Technology, Guiyang 550025, China
* Correspondence: dwkong@gzu.edu.cn

Abstract: The single-factor experiments are designed to quantitatively investigate the effects of silica fume, mineral powder, and fly ash on the mechanical and thermal insulation properties of desulfurization gypsum-based composites (DGCs). The effect mechanism is discussed from the microscopic morphology of the internal structure, and the corresponding relationship between the strength and thermal conductivity of this material is evaluated by the regression model. The results show that the admixture of silica fume, mineral powder, and fly ash improves the strengths and thermal insulation properties of DGCs, with the order of influence silica fume > mineral powder > fly ash. The optimal 28 d compressive strength and thermal conductivity are 34.17 MPa and 0.2146 W/(m·K), respectively, at a silica fume dosage of 35%. The enhancement effects on the strength and thermal insulation performance of DGCs are attributed to the increase in the hydration products C-S-H gel and Aft. Moreover, the thermal conductivity linearly decreases with the increase in the compressive strength of DGC after adding silica fume, mineral powder, and fly ash. The linear regression models exhibit good precision for evaluating the corresponding relationships between the compressive strength and thermal conductivity of DGCs with different admixtures.

Keywords: desulfurization gypsum; admixture; compressive strength; thermal conductivity; regression model

1. General Introduction

1.1. Introduction

Desulfurization gypsum is an industrial by-product produced during the process of wet flue gas desulfurization using limestone–gypsum in coal-fired power plants, and its main component is calcium sulfate dihydrate ($CaSO_4 \cdot 2H_2O$). Compared with natural gypsum, desulfurization gypsum has a more stable composition with smaller particle size and less harmful impurity content as well as high purity [1,2]. In China, a large number of coal-fired power plants are equipped with desulfurization facilities, causing the increased production of industrial by-product desulfurization gypsum. Additionally, the low utilization of desulfurization gypsum has brought many problems, such as land occupation and environmental pollution [3–5]. Therefore, the utilization and emission of desulfurization gypsum has become an urgent problem to be solved [6], and more approaches and channels to enhance the utilization of desulfurization gypsum resources need to be developed.

Silica fume, mineral powder, and fly ash are all large-scale industrial solid wastes, which can be ground into powder form and mixed with gypsum to prepare composite cementitious materials [7]. Among them, mineral powder has a similar chemical composition

to ordinary silicate cement and has similar self-hydration and self-hardening characteristics. It can partially replace cement and can exist in the form of microaggregates in the matrix of the materials to improve the pore structures, forming a high-quality admixture and cement mixing material. The active components contained in these admixtures, such as SiO_2 and Al_2O_3, undergo volcanic ash reaction under an alkaline environment, thereby modifying the properties of composite materials. The degree of activity is influenced by the type and content of different admixtures [8,9]. Therefore, the additions of silica fume, mineral powder, and fly ash are feasible approaches to improve the properties of desulfurization gypsum materials. The effect investigations of these admixtures on mechanical and thermal performances of desulfurization gypsum materials need to develop comprehensively. These results can provide the foundations for the applications of these solid wastes in large quantities and for reduction in the building energy consumption.

The present study adds silica fume, mineral powder, and fly ash into the matrix composed of cement and the original desulfurization gypsum modified by a small amount of semi-hydrated desulfurization gypsum. Desulfurization gypsum-based composites (DGCs) are prepared single-factor experiments are designed to investigate the effects of different admixtures on the mechanical and thermal properties of DGCs. The effect mechanism is discussed from a microscopic perspective of the DGC specimen. The results can provide more references for the large-scale applications of desulfurization gypsum in wall insulation materials.

1.2. Literature Review

Many investigations have been carried out to improve the performances of desulfurization gypsum by adding admixtures and catalysts to expand its large-scale usage in civil engineering and construction [10,11]. Wan et al. [12] explored the incorporation of ordinary silicate cement and fly ash into flue gas desulfurization (FGD) gypsum to develop a green binder and discussed the effect of the dosage of silicate cement and fly ash in order to reduce the cement dosage in structural engineering. Zhou et al. [2] utilized the response surface methodology (RSM) to investigate the effect factors of FGD gypsum-based composite cementitious materials. The results showed that this composite exhibited excellent strength and water resistance when the dosage of sulfated aluminate cement, mineral powder, and quick lime were 7.82%, 21%, and 5.22%, respectively. Zhao et al. [13] used the response surface method to obtain the optimal proportion ratio of underground backfilling materials with solid waste. The optimal ratio is coal gangue: fly ash: desulfurization gypsum: gasification fine slag: furnace bottom slag = 1:0.4:0.2:0.1:0.1. He et al. [14] studied the dosage effect of sodium methyl silicate on the water resistance of desulfurization gypsum block and elaborated the effect mechanism from a microscopic perspective. Many other scholars [15–17] have also chosen a specific admixture (e.g., silica fume, mineral powder, fly ash, etc.) and added it to desulfurization gypsum to make multi-system cementitious materials, so as to explore the role of the admixture in the composite system and its effects on the overall performance of the composite. However, these studies mainly focus on the effects of the admixture dosages on the performances of FGD gypsum. Therefore, it is difficult to determine the optimal admixture for FGD gypsum, because there is no scientific rigorous comparison of the effects of other active mineral admixtures on the properties of FGD gypsum.

The existing research mainly concentrates on the mechanical properties of modified desulfurization gypsum, but fewer studies are conducted on its thermal conductivity properties. Actually, the large porosity in desulfurization gypsum material results in small thermal conductivity and large hygroscopicity. Thus, the desulfurization gypsum is compatible with application in the wall insulation material to reduce the energy consumption of the building. Therefore, more investigations should be developed to improve the thermal insulation performance of desulfurization gypsum. Zhou et al. [18] added desulfurization gypsum in a paraffin/expanded perlite insulation mortar to improve the heat preservation and storage/exothermic properties of walls. The thermal conductivity of this material

was 0.076 W/(m·K) when the mass ratio of paraffin to expanded perlite was 6:4 and the mass ratio of composite phase change material to desulfurization gypsum was 1:3. Li et al. [19] modified desulfurized gypsum insulation materials by using hydrogen peroxide as the foaming agent, and glass fibers were added to improve their thermal properties. The corresponding results showed that the minimum thermal conductivity was 0.051 W/(m·K) when the dosage of the foaming agent was 4%. However, the addition of foaming agents led to poor mechanical properties of the matrix, and the 7 d compressive strength was less than 1 MPa. Lei et al. [20] added polystyrene particles into the desulfurization gypsum cementitious system to prepare lightweight thermal insulation materials, modified by mixing cellulose ether, latex powder, and polypropylene fibers. It was found that the thermal conductivity dropped to the minimum value of 0.0407 W/(m·K) when the proportion of polystyrene particle was 85.3%; however, the compressive strength was only 0.18 MPa, which could not meet the specification requirements. Additionally, different lightweight fillers (e.g., expanded polystyrene (EPS) [21], low-density polyethylene (LDPE) [22], etc.) and different foaming processes (physical foaming, chemical foaming, or composite foaming [23]) have been utilized to prepare FGD gypsum-based composites [10,24]. The thermal conductivities of these FGD gypsum-based composites are influenced by the density of internal structures, and lightweight fillers enhance the thermal insulation properties of FGD gypsum-based composites. However, the current research primarily adds physical foaming and chemical foaming to improve the thermal insulation performance of desulfurization gypsum. Unfortunately, these additives have negative effects on the mechanical properties of desulfurization gypsum, limiting the application and promotion of desulfurization gypsum material. In addition, adding insulating aggregates improves the thermal insulation performance of desulfurization gypsum, but reduces the mechanical properties greatly. Therefore, based on the need to preserve the mechanical properties, it is particularly important to study the effects of admixture changes on the thermal insulation property of the desulfurization gypsum and to evaluate the relationship between strength and thermal conductivity.

2. Experiment

2.1. Raw Materials

The experimental DGCs are mainly composed of undisturbed desulfurization gypsum and semi-hydrated desulfurization gypsum mixed with P.O 42.5 ordinary silicate cement, quicklime, silica fume, mineral powder, fly ash, polycarboxylate acid type powder water reducer and retarder and other admixtures. The above-mentioned admixtures are all commercially available, and the undisturbed desulfurization gypsum is taken from the waste yard of Guizhou Jinyuanchayuan Power Generation Co., Ltd., Guiyang, China; it is yellowish brown in color and needs to be crushed using a crusher and sieved through a 0.15 mm square hole. Then, the undisturbed desulfurization gypsum is calcined in an oven at 180 °C for 2 h, sealed and aged for 5–7 d to obtain the semi-hydrated desulfurization gypsum [2]. The chemical components of the raw materials are listed in Table 1. The high-performance polycarboxylate acid water reducer (powder) is produced by Gongyi Longze Water Purification Material Co., Ltd., Zhengzhou, China and the gypsum retarder (CQ-SHJ09 type) is from Shanghai Chenqi Chemical Technology Co., Ltd. Shanghai, China.

Table 1. The chemical compositions of the raw materials.

Raw Materials	SO$_3$	CaO	SiO$_2$	Al$_2$O$_3$	Fe$_2$O$_3$	K$_2$O	P$_2$O$_5$	F	MgO
Undisturbed desulfurization gypsum	53.416	40.21	3.31	1.324	0.538	0.241	0.03	0.862	-
Semi-hydrated desulfurization gypsum	54.851	38.506	2.859	1.108	0.470	0.232	0.027	0.744	-
Cement	3.962	61.713	19.897	5.155	4.456	1.196	0.169	-	1.725
Silica fume	0.455	0.484	97.598	0.809	0.070	0.221	0.041	-	0.207
Quick lime	0.292	96.775	0.520	0.154	0.115	0.011	0.003	-	2.051
Mineral powder	2.609	35.179	34.985	15.703	0.842	7.582	0.025	-	-
Fly ash	5.220	98.290	49.100	36.870	3.130	0.980	0.400	-	0.680

2.2. Experimental Design and Method

The matrix materials consist of undisturbed desulfurization gypsum and semi-hydrated desulfurization gypsum (70:30); DGCs are obtained by adding and mixing 10% cement, 3% quicklime, and 1% water reducer as well as 0.2% retarder, and their water-gypsum ratio is fixed at 0.28. On this basis, the dosages of silica fume, mineral powder, and fly ash are considered as variables to design experiments of different matching ratios by using the external doping method. The compositions of each set of samples are listed in Table 2. After mixing the admixtures well, the test specimens are prepared and maintained according to the conditions specified in the "Test Method for Cementitious Sand Strength (ISO Method)" (GB/T 17671-1999) and "Determination of Steady State Thermal Resistance and Related Characteristics of Insulating Materials: Protective Heat Plate Method" (GB/T 10294-2008), in which the test specimen used to determine mechanical properties is 40 mm × 40 mm × 160 mm, and the size of the test specimen used to measure thermal conductivity is 300 mm × 300 mm × 30 mm. The corresponding specimens are removed from the molds after 24 h of curing in a natural environment. The test specimens are all cured at 20 ± 3 °C and 50 ± 5% relative humidity until the corresponding age. In addition, the thermal conductivity of the specimen is tested using a CD-DR3030 thermal conductivity tester. The allowable thermal conductivity error of the instrument is 3%, and the instrument and standard specimen are shown in Figure 1. Moreover, the electron microscopic scanning is performed with a TESCAN (Brno, Czech Republic) MIRA LMS model instrument to obtain the microscopic morphology on the fracture surfaces of selected specimens.
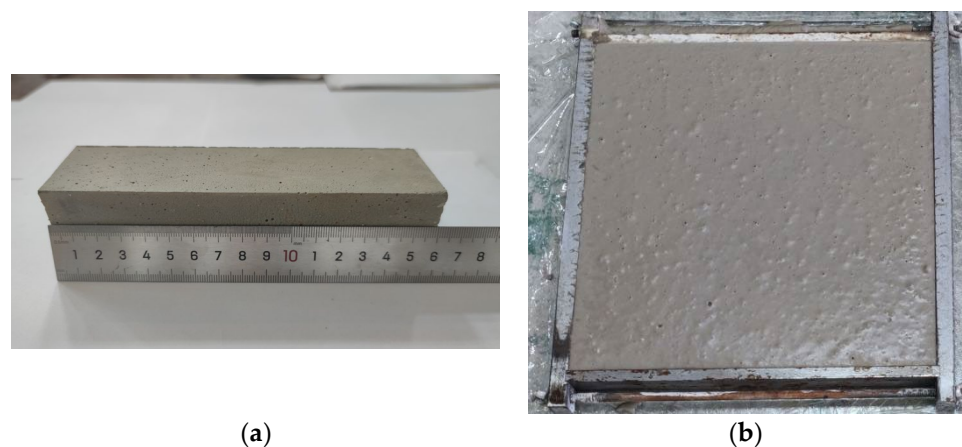

(**a**)　　　　　　　　　　　　(**b**)

Figure 1. The specimens used for the measurement of mechanical properties and thermal conductivity. (**a**) Standard specimen to determine mechanical properties. (**b**) Standard specimen to determine thermal conductivity.

Table 2. Single-factor tests mix ratio (wt.%).

Undisturbed/ Semi-Hydrated Desulfurization Gypsum	Silica Fume (%)	Mineral Powder (%)	Fly Ash (%)	Cement (%)	Quicklime (%)	Water Reducer (%)	Retarder (%)
70:30	15, 20, 25, 30, 35	0	0	10	3	1	0.2
70:30	0	10, 15, 20, 25, 30	0	10	3	1	0.2
70:30	0	0	8, 13, 18, 23, 28	10	3	1	0.2

3. Results and Discussion

3.1. Effects of Silica Fume Dosage on the Performances of DGCs

Silica fume (SF) with small granularity, lighter quality, and high activity is a dust-collecting powder used during the process of smelting industrial silicon and ferrosilicon. Compared with other mineral admixtures, silica fume exhibits a better micro-aggregate effect on cementing materials and a faster reaction with volcanic ash [25,26]. The pre-experiments were conducted with a silica fume dosage gradient of 10% to measure the compressive property, determining the reasonable dosage range of silica fume from 15% to 35%. Then, the effect of SF dosage on the performance of DGCs was investigated under a dosage gradient of 5%, as the other admixtures were unchanged. The performances of DGCs under different silica fume dosages are given in Figure 2.
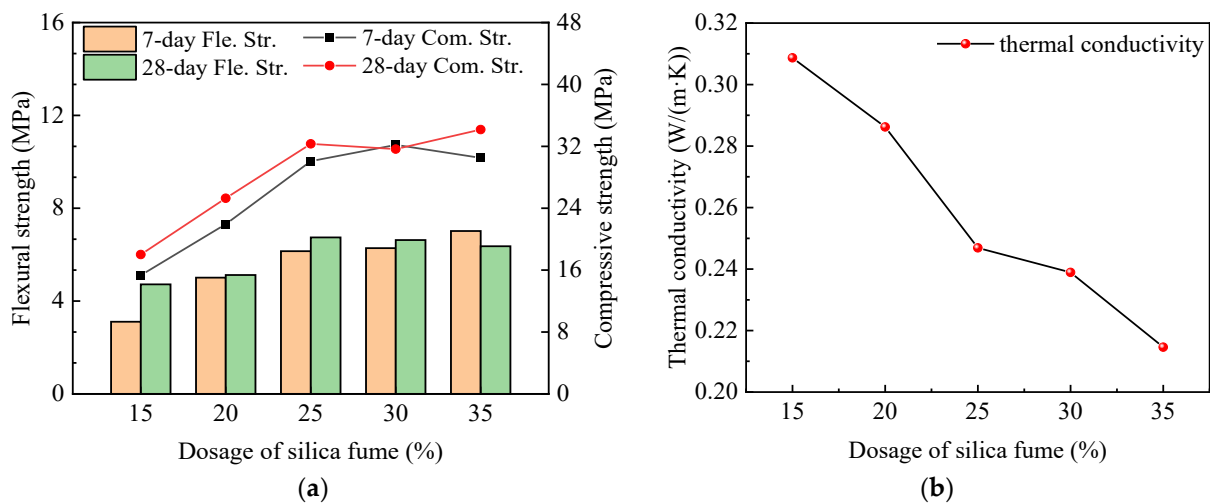

Figure 2. Effects of different silica fume dosage on the performance of DGCs. (**a**) Mechanical properties; (**b**) Thermal insulation performance.

Figure 2a gives the effect of SF dosage on the flexural and compressive strength of this cementitious material. It can be seen that the 7 d absolute dry flexural strength increases with the increase in SF dosage, and reaches a maximum value of 7.02 MPa at the SF dosage of 35%. The 28 d absolute dry flexural strength increases and then decreases with the increase in SF dosage, and the absolute dry flexural strength reaches a maximum value of 6.74 MPa at the SF dosage of 25%. This is because the main component of SF is indeterminate SiO_2, with strong volcanic ash activity and an effect on filling density [27]. It reacts with $Ca(OH)_2$ in an alkaline environment to generate water-insoluble hydrated calcium silicate, and gradually coalesces into a gel (C-S-H gel). The SEM images of DGCs with different dosages of SF are shown in Figure 3. As in Figure 3a, the precipitated crystals lap through each other to form a hard skeleton structure, so as to improve the early flexural strength. However, with the increase in SF dosage, more hydration heat is released from the secondary hydration reaction, and the temperature stress causes cracks in the specimens, resulting in a later reduction in flexural strength. The variation

in compressive strength at 7 d and 28 d tends to rise first and then level off with the increase in SF dosage, and the 28 d compressive strength is generally higher than the 7 d compressive strength. This is attributed to the SF and $Ca(OH)_2$, the hydration product of cement and quicklime, generating the gel by volcanic ash reaction. Additionally, the silica fume particles and products of the volcanic ash reaction fill the pores of the gel, as shown in Figure 3b, strengthening the internal structure. In addition, the increase in time and dosage accelerates the secondary hydration reaction of SF, improving the hydration conditions of cement and promoting the hydration process of the cementitious system. Therefore, the improvement in 28 d compressive strength is more obvious compared to that at 7 d. However, SF, with a small particle size and a large specific surface area, exhibits a strong water absorption effect. When the SF is excessive, it absorbs water and forms a silica-rich gel to cover and wrap the un-hydrated cement particles [28], inhibiting the complete hydrated of the cement and the hydration of the cementitious system. These actions led to a slow rise and even a decrease in the compressive strength of the DGC specimens.
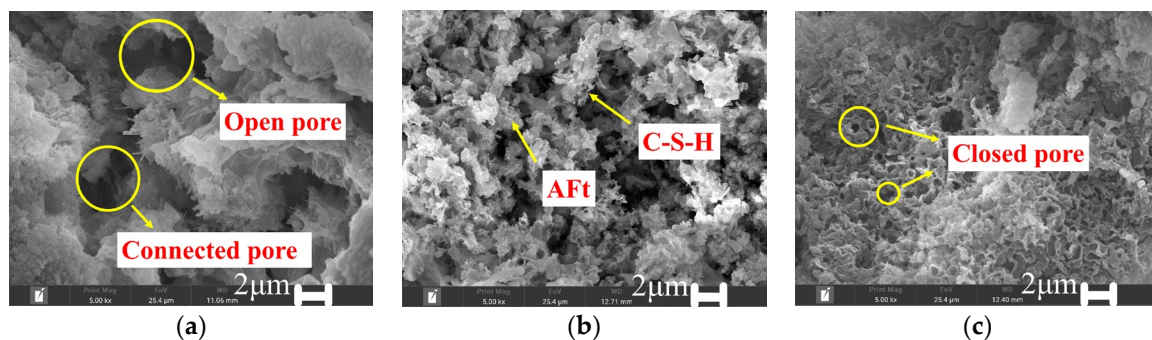

Figure 3. Micrographs of DGCs under different dosages of silica fume: (**a**) 15%; (**b**) 25%; (**c**) 35%.

The effect of SF dosage on the thermal conductivity of DGC is shown in Figure 2b. From the figure, it can be seen that the thermal conductivity of the cementitious material decreases with the increase in SF dosage, and decreases from 0.3087 to 0.2146. When the low dosage of SF is added to the porous DGC structure, less silica fume participates in the hydration reaction and fewer hydration products are generated. No hydration product is connected in the gypsum matrix, so the internal structure is mostly connected pores and open pores, as shown in Figure 3a. Meanwhile, the influence of the pore structure on the thermal conductivity is dominant, and air convection occurs in these connected pores, causing high thermal conductivity. However, with the increase in SF dosage, the hydration products increase, and the formed cementitious systematic mesh structure is supplemented by hydration products and C-S-H gels. The coarse pores are also separated into smaller pores and closed pores, as in Figure 3b, leading to a decrease in thermal conductivity. Moreover, as the SF dosage increases to 35%, more pores and smaller pore sizes are observed, as shown in Figure 3c, which prevent heat transfer. Summarily, with the increase in the SF dosage, the thermal conductivity of DGC decreases and its thermal insulation performance improves.

It is clearly observed from Figure 3 that only Aft (a hydration product of cement in the form of needle-like crystals) and a small amount of gel are generated when the SF dosage was 15%. These hydration products do not mutually overlap with each other, resulting in larger pores inside the structure, as shown in Figure 3a. Additionally, when the SF dosage increases to 35%, the relative decrease in the water-cement ratio leads to the generation of more C-S-H gel and more crystals of hydration products. They attach to the surface of the gypsum and connect mutually, which continuously strengthens the dense spatial mesh structure, as seen in Figure 3c. As a result, the mechanical properties and thermal insulation performance of the materials are improved.

3.2. Effects of Mineral Powder on the Performances of DGCs

Mineral powder is also known as slag micro powder, ground granulated blast-furnace slag (GGBS), which is generated from the process of crushing and processing ores. The mineral powder can be used as an admixture without calcination in the production process, thus having better environmental and economic benefits. The vast majority of its particles are overwhelmingly vitreous, with its main active ingredients being Al_2O_3 and SiO_2, so it potentially has high activity [29,30]. The effects of GGBS dosages on the mechanical and thermal conductivity of DGCs are summarized in Figure 4, and the microscopic morphologies of fractures under different GGBS dosages are provided in Figure 5.
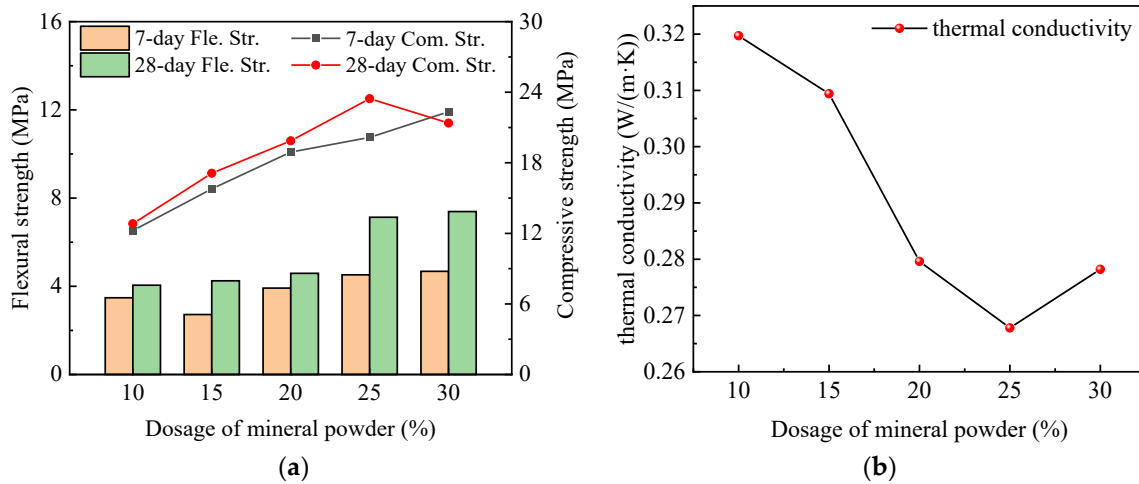

(a)

(b)

Figure 4. Effects of different mineral powder dosages on the performances of DGCs. (**a**) Mechanical properties; (**b**) Thermal insulation performance.
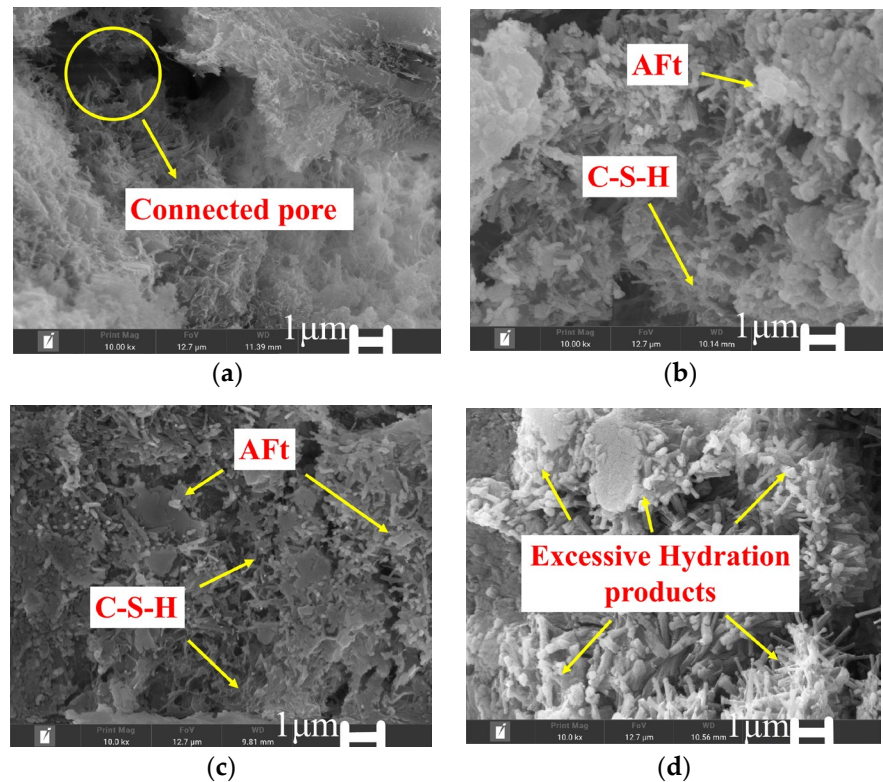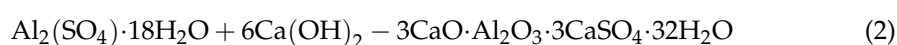

(a)

(b)

(c)

(d)

Figure 5. Micrographs of DGCs under different dosages of mineral powder. (**a**) 10%; (**b**) 20%; (**c**) 25%; (**d**) 30%.

Figure 4a indicates that the 7 d and 28 d flexural strength of the cementitious materials exhibit an uptrend at the beginning, while the flexural strength grows slowly with the increase in GGBS dosage at the latter period. Additionally, the 7 d compressive strength increases linearly, whereas the 28 d compressive strength increases first and then decreases, reaching the maximum of 23.45 MPa at the GGBS dosage of 25%. This is because GGBS is weakly water hardened, and its activity is only stimulated by the alkaline environment provided by lime, cement, and other alkaline activators and under the action of sulfate activators such as undisturbed desulfurized gypsum and semi-hydrated desulfurized gypsum, contributing to the hydration reaction [29]. This process produces C-S-H gels and calcium alumina (AFt), a hydration product in the form of needle-like crystals, which greatly enhances the strength of the cementitious materials. The reactions are shown in the following equations [2]:

$$Ca^{2+} + SiO_3^{2-} + 3H_2O = CaO \cdot SiO_2 \cdot 3H_2O \tag{1}$$

$$Al_2(SO_4) \cdot 18H_2O + 6Ca(OH)_2 - 3CaO \cdot Al_2O_3 \cdot 3CaSO_4 \cdot 32H_2O \tag{2}$$

However, excessive GGBS reacts with gypsum to produce excessive AFt, and the gypsum setting and hardening rates are faster than the hydration reaction rate of Aft production. This causes AFt to squeeze gypsum from the inside during the maintenance process, generating expansion stresses. The corresponding expansion of the cementitious material causes cracks in the structure, resulting in a reduction in strength [31,32].

The effect of GGBS dosage on the thermal conductivity of DGCs is shown in Figure 4b, which specifically shows that its thermal conductivity first decreases and then increases, and reaches a minimum value of 0.2678 W/(m·K) at 25%. This is because the increasing GGBS admixture accelerates the hydration reaction of GGBS and cement; thus, the water is consumed rapidly to form closed pores. In addition, the increase in C-S-H gel and AFt generated from the admixture interaction improves the pore state of the matrix, as shown in Figure 5a–c, limiting the thermal convection of air in the pores inside the matrix, which is macroscopically manifested by the decrease in thermal conductivity. On the contrary, as the GGBS dosage continues to increase, the excess generated AFt crystals pile up closely and extrude each other, as seen in Figure 5d. The bulk density of the specimens becomes larger and the contact points of the internal structure increase, which reduces the heat transfer resistance and increases the thermal conductivity of the material [33]. As shown in Figure 5a, at a GGBS dosage of 10%, a reduction in hydration reaction products which partially cover the surface of the gypsum occurs, and many gaps within the gypsum structure are observed. With the increase in dosage, abundant C-S-H gel and AFt are generated in large quantities, and the gathered gels and the penetrated and lapped AFt between the matrix fill and densify the space structure as seen in Figure 5b–c. At a GGBS dosage of 30%, Figure 5d shows that greater amounts of hydration products in crystal form precipitate and wrap around the surface of the gypsum, interacting to swell the matrix and produce stress concentration. This phenomenon is the main reason for the reduction in strength.

3.3. Effects of Fly Ash on the Performances of DGCs

Fly ash (FA), as a by-product of coal-fired power plant processing, is composed of tiny ash particles, with smooth spherical shape and weak, water-hardened cementitious properties, whose activity mainly depends on the vitreous content [34,35]. Under the constant dosages of other admixtures, the variations of mechanical and thermal insulation properties of DGCs with FA dosages are shown in Figure 6, and the microscopic morphologies of DGCs with different FA dosages are given in Figure 7.
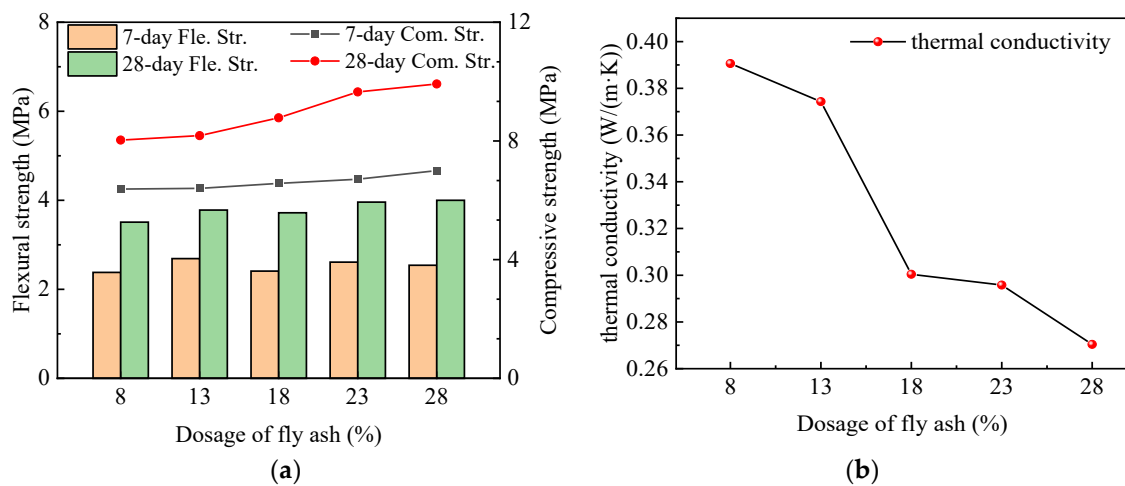
Figure 6. Effects of different fly ash dosages on the performances of DGCs. (**a**) Mechanical properties; (**b**) Thermal insulation performance.
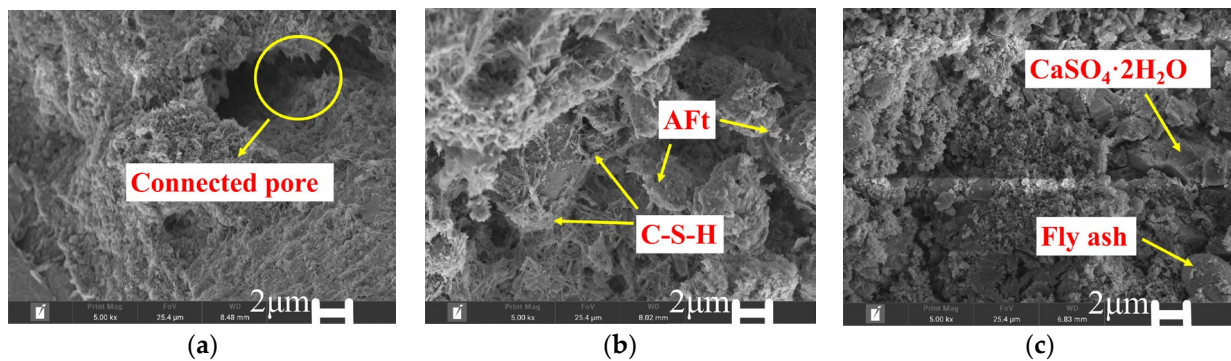

Figure 7. Micrographs of DGCs under different dosages of fly ash. (**a**) 8%; (**b**) 18%; (**c**) 28%.

From Figure 6a, the 7 d flexural strength of the specimens fluctuates up and down, but overall remains at about 2.5 MPa. The 28 d flexural strength improves and exhibits a similar overall trend as the 7 d flexure strength. The 7 d compressive strength exhibits a slight raise with the increase in FA dosage, and the maximum value is 7 MPa at an FA dosage of 28%. The 28 d compressive strength shows a significant increase, and the increase rate with 18%–28% dosage is higher than the rate with 8%–18% dosage. Additionally, Figure 6b indicates the thermal conductivity exhibits an integral decreasing trend, with the increase in the FA dosage ranging from 13% to 18%. This is because compared with silica fume and mineral powder, the FA exhibits weaker activity, mainly showing a dilution effect and nucleation effect at the initial period. As a result, the volcanic ash has a less obvious effect on the hydration reaction, causing a large number of pores inside the DGC structure, as shown in Figure 7a. Thus, the heat is less impeded in the transfer process [36], leading to high thermal conductivity. Consequently, DGC with 8% FA dosage has relatively low strength and high thermal conductivity. However, as FA dosage increases to 18%, FA begins to undergo significant hydration reactions after 7 days [37], and Al_2O_3 and SiO_2 in FA react with $Ca(OH)_2$ produced by the initial hydration. It is found in Figure 7b that the water-hardening products C–S(A)–H and AFt are generated in the secondary hydration reactions, enhancing strength in later stages. Moreover, as the FA dosage increases to 28%, the free water and $Ca(OH)_2$ are continuously consumed by the hydration reaction, which reduces the alkalinity of the solution and inhibits the reaction of volcanic ash. The effective reaction of a small amount of FA causes the unreacted FA to just fill in the pores, as shown in Figure 7c; therefore, the strengths of DGCs exhibit a slight increase from the FA dosage of 23% to 28%. Additionally, the filling phenomenon of untreated FA reduces

the number of open pores and connecting pores, but increases the number of closed pores. Thus, the heat is transferred alternately between the gypsum solid and the gas in the closed pores, causing partial heat loss. Furthermore, FA has lower thermal conductivity than cementitious materials. Consequently, the thermal conductivity of DGC exhibits a continuous decrease with the increase in FA dosage from 8% to 28%.

3.4. Effect Comparisons of Different Admixtures

The effects of silica fume, mineral powder, and fly ash on the strengths and thermal conductivity of DGCs are individually discussed in Sections 3.1–3.3. Experimental results show that three admixtures have significant effects on the mechanical properties and thermal resistance of DGC. The effect comparisons of different admixtures on the 28 d strength and thermal conductivity of DGC are summarized in Figure 8.
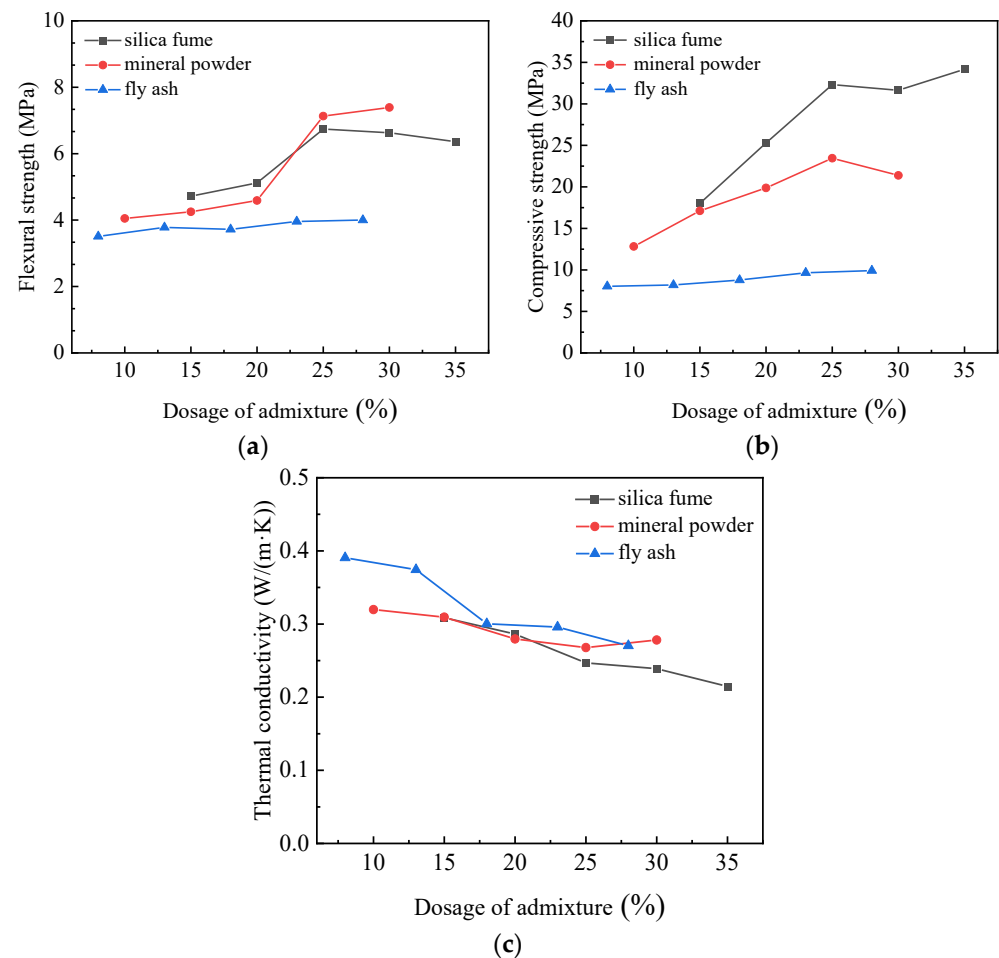

Figure 8. Effect of different admixtures on the mechanical and thermal conductivity of DGCs. (**a**) Effects of different admixtures on the 28 d flexural strength of DGC; (**b**) Effects of different admixtures on the 28 d compressive strength of DGC; (**c**) Effects of different admixtures on the thermal conductivity of DGC.

It can be found in Figure 8a that silica fume and mineral powder exhibit more obvious enhancement effects on the flexural properties of DGCs than fly ash. However, compared with mineral powder, silica fume has a better enhancement effect on flexural strength below the dosage of 23%, but a weaker enhancement effect above the dosage of 23%. Additionally, silica fume has the most significant enhancement effect on the compressive strength of DGC compared with the other two admixtures, and this enhancement effect becomes more and more obvious with the increase in the dosage. Similarly to the flexural strength, the compressive strength of the DGC exhibits a slight dependence on the dosage of fly ash.

In Figure 8c, thermal conductivity of DGC with added fly ash is higher than those of silica fume and mineral powder, when the dosage is less than 25%. Above the dosage of approximately 20%, the thermal conductivity of DGC with silica fume decreases with the increase in the dosage, and is lower than those of DGCs with adding mineral powder and fly ash. The comparisons in Figure 8b,c state that silica fume can better increase the compressive strength and thermal insulation performance of DGC. This is attributed to the low fineness and good physical form of silica fume, refining the crystal pore size and optimizing the internal pore structure of the matrix after maintenance. Moreover, with the addition of silica fume with a high content of amorphous SiO_2 and strong volcanic ash activity, the hydration reaction occurs thoroughly at the beginning of maintenance [38]. In contrast, the low activity of fly ash causes a slow rate of hydration reaction and a weak volcanic ash effect in the early period. Meanwhile, a small amount of FA participates in the hydration reaction [37], and FA plays a filling role with an increase in its dosage, which lead to a looser structure of the matrix compared with silica fume. The looser structure results in a slight enhancement in the strength and high thermal conductivity. Additionally, the mineral powder has better potential activity than fly ash, which is easily excitable in an alkaline environment and shows better cementation in the state of a strongly alkaline solution [39]. As an alkaline exciter, quicklime provides an alkaline environment to stimulate the activity of materials and promote hydration and adsorption of impurities. However, excessive quicklime reacts to generate a large amount of white solid $CaCO_3$, which causes expansion and cracking in the DGC specimen during the maintenance period. Therefore, the compressive strength and thermal insulation of DGC with mineral powder decrease from the dosage of 25% to 30%.

The Archimedes method is used to measure the porosity, and the formula is as follows:

$$P = (W_{sat} - W_d)/(W_{sat} - W_{sum}) \times 100\% \tag{3}$$

where W_{sat} is the saturated weight of the specimen, W_d is the dry weight of the specimen, and W_{sum} is the suspended weight in water. P is the porosity of the DGCs [8].

Table 3 gives the porosity of DGCs with different admixtures and dosages, and the formula for calculating the porosity is shown in Equation (3). It can be seen from the data in the table that the porosity decreases continuously with the increase in admixtures. This is attributed to the fact that with the increase in the dosage, the hydration products are constantly generated, and the space inside the matrix is continuously supplemented and perfected by these hydration products, so the porosity shows a decreasing trend. On the one hand, the reduced porosity provides a denser internal structure for the improvement of mechanical properties of DGCs. On the other hand, combined with the electron micrographs, it is clear that the reduction in porosity is mainly caused by the reduction in the number of larger open and connected pores, and these large pores become denser, closed pores with the reduction in porosity, improving the pore structures and providing a good internal environment for the thermal conductivity. Moreover, the porosities of DGCs with different admixtures are ranked from small to large as silica fume < mineral powder < fly ash, which also maintains a good correspondence with the rankings of mechanical properties and thermal conductivity of DGCs.

Table 3. Effects of different admixtures on the porosity of DGCs.

Dosage of Silica Fume (%)	15	20	25	30	35
Porosity (%)	13.42	12.67	12.51	12.26	11.78
Dosage of mineral powder (%)	10	15	20	25	30
Porosity (%)	18.96	18.31	17.23	16.39	14.59
Dosage of fly ash (%)	8	13	18	23	28
Porosity (%)	20.77	19.31	19.54	18.61	17.36

In conclusion, silica fume, mineral powder, and fly ash exhibit enhancement effects on the flexural and compressive strength of DGCs, as well as a reduction effect on the thermal conductivity. However, the three admixtures have different effect rules owing to their different physical and chemical properties. Micrographs of DGCs show that different hydration reactions of the DGCs and hydration products change the internal structure of the matrix, affecting the strength and thermal conductivity of the DGC.

3.5. Regression Analysis of Compressive Strength and Thermal Conductivity

The effects of different admixtures on DGCs show that the compressive strength and thermal conductivity have a corresponding variation relationship. The increase in the compressive strength and decrease in the thermal conductivity is attributed to the effects of morphology and hydration products. Therefore, the relationship between compressive strength and thermal conductivity of DGC can be quantitatively evaluated to improve experimental efficiency. The regression analysis and significance test of the experimental results are performed using SPSS software in this paper [40]. The regression prediction models are as follows:

$$y_i = k_1 x_i + k_2$$

where y_i (i = 1, 2, 3) are the measured values of thermal conductivities (W/(m·K)) of DGCs reinforced with silica fume, mineral powder, and fly ash, respectively. x_i (i = 1, 2, 3) denotes the experimental values of compressive strengths (MPa) of DGCs with silica fume, mineral powder, and fly ash, respectively. k_1 and k_2 are the coefficients of regression equations, and the regression coefficients of different models are listed in Table 4.

Table 4. Regression fitting coefficients for each model.

Coefficient	y_1	y_2	y_3
k_1	−0.005	−0.005	−0.058
k_2	0.414	0.390	0.841

From Table 5, it can be seen that the R^2 value of each model is close to 1, indicating a high fitting precision. Moreover, the significant experimental values of each model in Table 6 are less than 0.05, which denotes the statistical significance and remarkable effect of the regression models [41].

Table 5. Model Summary.

Model	R	R^2	Adjusted R^2	Errors in Standard Estimation
1	0.964	0.928	0.905	0.0116912
2	0.966	0.934	0.912	0.0066251
3	0.931	0.867	0.822	0.0222666

Table 6. Analysis of variance.

Model	-	Quadratic Sum	Degree of Freedom	Mean Square	F Value	Significance
	Regression	0.005	1	0.005	38.934	0.008
1	Residual error	0	3	0	-	-
	Grand total	0.006	4	-	-	-
	Regression	0.002	1	0.002	42.436	0.007
2	Residual error	0	3	0	-	-
	Grand total	0.002	4	-	-	-
	Regression	0.01	1	0.01	19.518	0.022
3	Residual error	0.001	3	0	-	-
	Grand total	0.011	4	-	-	-

Figure 9 provides comparisons between experimental and prediction values, in which the experimental and predicted values are evenly distributed near the regression line. The comparisons show good agreement and indicate that this regression model can be utilized for the optimization of the compressive strength and thermal conductivity of DGCs.
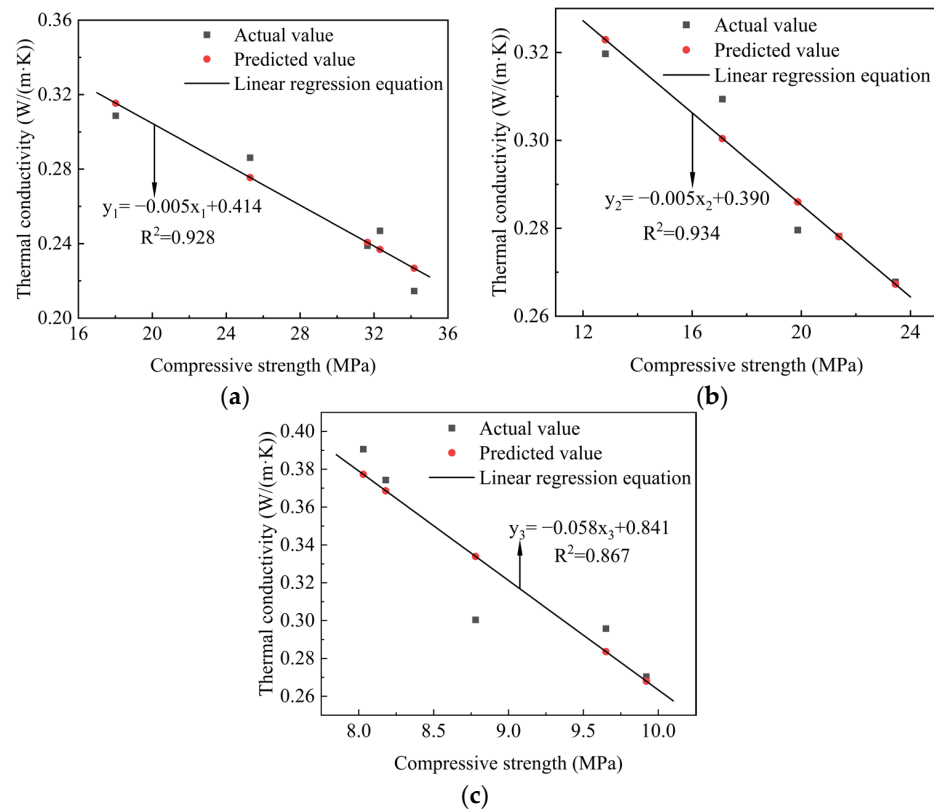

Figure 9. Comparisons between actual and predicted values of compressive strength and thermal conductivity. (**a**) DGC with silica fume; (**b**) DGC with mineral powder; (**c**) DGC with fly ash.

4. Conclusions

In this study, the enhancement effects of silica fume, mineral powder, and fly ash on mechanical properties and thermal insulation properties of DGCs are investigated using experimental approaches. The effects of dosages of different admixtures on flexural strength, compressive strength, and thermal conductivity are discussed, and the action mechanism of different admixtures is revealed from the microscopic perspective. The regression models are established to evaluate the corresponding relationship between compressive strength and thermal conductivity. The main conclusions are summarized as follows:

Under the present test conditions, the incorporation of silica fume, mineral powder, and fly ash significantly enhances the mechanical properties of DGCs while also effectively improving their thermal insulation properties. Among them, the compressive strength and thermal conductivity of DGCs with 35% silica fume admixture are the best, which are 34.17 MPa and 0.2146 W/(m·K), respectively.

Based on the results of the comparative analysis, the degree of influence of different admixtures on the mechanical properties and thermal conductivity of DGCs is silica fume > mineral powder > fly ash in descending order. The differences are mainly due to the variation of physical and chemical properties of different active admixtures, which have different degrees of influence on the hydration reaction and microstructure of DGCs.

The mechanism of different admixtures on the improvement in the strength and thermal insulation performance of DGCs is mainly as follows: the increase in hydration products C-S-H gel and AFt leads to the enhancement of the denseness of the internal struc-

ture of the matrix, which improves the compressive strength. Meanwhile, the formation of hydration products optimizes the pore structure and transforms the connected pores and open pores into closed pores, which hinder the heat transfer, thus improving the thermal insulation performance.

The linear regression models exhibit good precision for evaluating the corresponding relationship between compressive strength and thermal conductivity in DGCs with different admixtures. The thermal conductivity linearly decreases with the increase in the compressive strength of DGC with silica fume, mineral powder, and fly ash. The regression models show high correlation coefficients, obvious significance and good fitting, and can be used to optimize the compressive strength and thermal conductivity of DGCs.

References

1. Wang, S.J.; Chen, Q.; Li, Y.; Zhuo, Y.Q.; Xu, L.Z. Research on saline-alkali soil amelioration with FGD gypsum. *Resour. Conserv. Recycl.* **2017**, *121*, 82–92. [CrossRef]
2. Zhou, Y.; Xie, L.; Kong, D.; Peng, D.; Zheng, T. Research on optimizing performance of desulfurization-gypsum-based composite cementitious materials based on response surface method. *Constr. Build. Mater.* **2022**, *341*, 127874. [CrossRef]
3. Yuwei, Z.; Wenmin, Q.; Pengxiang, Z.; Yu, L.; Xiaoli, L.; Bin, L.; Ping, N. Research on red mud-limestone modified desulfurization mechanism and engineering application. *Sep. Purif. Technol.* **2021**, *272*, 118867.
4. Zeng, L.-L.; Bian, X.; Zhao, L.; Wang, Y.-J.; Hong, Z.-S. Effect of phosphogypsum on physiochemical and mechanical behaviour of cement stabilized dredged soil from Fuzhou, China. *Geomech. Energy Environ.* **2021**, *25*, 100195. [CrossRef]
5. Zhou, J.; Ding, B.; Tang, C.; Xie, J.-B.; Wang, B.; Zhang, H.; Ni, H. Utilization of semi-dry sintering flue gas desulfurized ash for SO₂ generation during sulfuric acid production using boiling furnace. *Chem. Eng. J.* **2017**, *327*, 914–923. [CrossRef]
6. Liu, S.; Liu, W.; Jiao, F.; Qin, W.; Yang, C. Production and resource utilization of flue gas desulfurized gypsum in China—A review. *Environ. Pollut.* **2021**, *288*, 117799. [CrossRef]
7. Wu, H.; Jia, Y.; Yuan, Z.; Li, Z.; Sun, T.; Zhang, J. Study on the Mechanical Properties, Wear Resistance and Microstructure of Hybrid Fiber-Reinforced Mortar Containing High Volume of Industrial Solid Waste Mineral Admixture. *Materials* **2022**, *15*, 3964. [CrossRef]
8. Xie, L.; Zhou, Y.; Xiao, S.; Miao, X.; Murzataev, A.; Kong, D.; Wang, L. Research on basalt fiber reinforced phosphogypsum-based composites based on single factor test and RSM test. *Constr. Build. Mater.* **2022**, *316*, 126084. [CrossRef]
9. Ai, Y.-P.; Xie, S.-K. Hydration Mechanism of Gypsum-Slag Gel Materials. *J. Mater. Civ. Eng.* **2020**, *32*, 04019326.
10. Yang, L.; Jing, M.; Lu, L.; Zhu, X.; Zhao, P.; Chen, M.; Li, L.; Liu, J. Effects of modified materials prepared from wastes on the performance of flue gas desulfurization gypsum-based composite wall materials. *Constr. Build. Mater.* **2020**, *257*, 119519. [CrossRef]
11. Gu, K.; Chen, B. Research on the incorporation of untreated flue gas desulfurization gypsum into magnesium oxysulfate cement. *J. Clean. Prod.* **2020**, *271*, 122497. [CrossRef]
12. Wan, Y.; Hui, X.; He, X.; Li, J.; Xue, J.; Feng, D.; Liu, X.; Wang, S. Performance of green binder developed from flue gas desulfurization gypsum incorporating Portland cement and large-volume fly ash. *Constr. Build. Mater.* **2022**, *348*, 128679. [CrossRef]
13. Zhao, X.; Yang, K.; He, X.; Wei, Z.; Zhang, J. Study on proportioning experiment and performance of solid waste for underground backfilling. *Mater. Today Commun.* **2022**, *32*, 103863. [CrossRef]
14. He, T.S.; Kang, Z.Q.; Chen, C. Influence of sodium methyl silicate on waterproof property of desulfurized gypsum block. *J. Build. Mater.* **2021**, *24*, 247–253+259. (In Chinese)

15. Duan, D.; Liao, H.; Wei, F.; Wang, J.; Wu, J.; Cheng, F. Solid waste-based dry-mix mortar using fly ash, carbide slag, and flue gas desulfurization gypsum. *J. Mater. Res. Technol.* **2022**, *21*, 3636–3649. [CrossRef]
16. Fu, Q.; Lian, F.; Lu, L.; Hu, S.; Zhao, Y.; Qin, J.; Wang, J. Recycling of ternary industrial by-products as cement replacement material and its influence on the durability of restored pavement potholes. *Road Mater. Pavement Des.* **2023**, *24*, 367–387. [CrossRef]
17. Li, J.; Cao, J.; Ren, Q.; Ding, Y.; Zhu, H.; Xiong, C.; Chen, R. Effect of nano-silica and silicone oil paraffin emulsion composite waterproofing agent on the water resistance of flue gas desulfurization gypsum. *Constr. Build. Mater.* **2021**, *287*, 123055. [CrossRef]
18. Zhou, Y.; Wang, S.X. Experimental Study on Composite Phase Change Thermal Insulation Mortar. *Key Eng. Mater.* **2020**, *6037*, 60–169. [CrossRef]
19. Lin, L.L.; Zhong, L.G. The Preparation of Modified Fiber Reinforced Desulfurization Gypsum Insulation Board. *Appl. Mech. Mater.* **2014**, *711*, 177–180.
20. Lei, D.Y.; Guo, L.P.; Sun, W. Preparation and performance of undisturbed FGD gypsum-based polystyrene lightweight thermal insulation material. *J. Southeast Univ.* **2017**, *47*, 384–391. (In Chinese) [CrossRef]
21. Shi, G.; Liu, T.; Li, G.; Wang, Z. A novel thermal insulation composite fabricated with industrial solid wastes and expanded polystyrene beads by compression method. *J. Clean. Prod.* **2021**, *279*, 123420. [CrossRef]
22. Bakshi, P.; Pappu, A.; Gupta, M.K.; Srivastava, A.K. Thermal Power Plant Flue Gas Desulfurization (FGD) Gypsum Waste Particulates Reinforced Injection Molded Flexible Composites. *J. Sci. Ind. Res.* **2021**, *80*, 612–616.
23. Liu, J.; Xie, H.; Wang, C.; Han, Y. Preparation of multifunctional gypsum composite with compound foaming process. *Powder Technol.* **2023**, *418*, 118289. [CrossRef]
24. Dolezelova, M.; Scheinherrova, L.; Krejsova, J.; Keppert, M.; Cerny, R.; Vimmrova, A. Investigation of gypsum composites with different lightweight fillers. *Constr. Build. Mater.* **2021**, *297*, 123791. [CrossRef]
25. Lou, Y.; Khan, K.; Amin, M.N.; Ahmad, W.; Deifalla, A.F.; Ahmad, A. Performance characteristics of cementitious composites modified with silica fume: A systematic review. *Case Stud. Constr. Mater.* **2023**, *18*, e01753. [CrossRef]
26. Senff, L.; Hotza, D.; Lucas, S.; Ferreira, V.M.; Labrincha, J.A. Effect of nano-SiO_2 and nano-TiO_2 addition on the rheological behavior and the hardened properties of cement mortars. *Mater. Sci. Eng. A* **2011**, *532*, 354–361. [CrossRef]
27. Long, G.C.; Wang, X.Y.; Xiao, R.M. Research of filling role of mineral blends in C3S cementitious system. *J. Build. Mater.* **2002**, *5*, 215–219. (In Chinese) [CrossRef]
28. Yazıcı, H.; Yiğiter, H.; Karabulut, A.Ş.; Baradan, B. Utilization of fly ash and ground granulated blast furnace slag as an alternative silica source in reactive powder concrete. *Fuel* **2008**, *87*, 2401–2407. [CrossRef]
29. Yalcinkaya, C.; Copuroglu, O. Hydration heat, strength and microstructure characteristics of UHPC containing blast furnace slag. *J. Build. Eng.* **2021**, *34*, 101915. [CrossRef]
30. Li, W.; Yi, Y.; Puppala, A.J. Effects of curing environment and period on performance of lime-GGBS-treated gypseous soil. *Transp. Geotech.* **2022**, *37*, 100848. [CrossRef]
31. MYin, G.; Wang, H.; Shi, F.T. Mechanical strength and pore structure analysis of modified phosphogypsum. *Mater. Rep.* **2018**, *32*, 526–529. (In Chinese)
32. Huntzinger, D.N.; Eatmon, T.D. A life-cycle assessment of Portland cement manufacturing: Comparing the traditional process with alternative technologies. *J. Clean. Prod.* **2009**, *17*, 668–675. [CrossRef]
33. Xi, Y.G.; Peng, T.J. Preparation and characterization of expanded vermiculite/gypsum thermal insulation composites. *Acta Mater. Compos. Sin.* **2011**, *28*, 156–161. (In Chinese) [CrossRef]
34. Duan, S.; Wu, H.; Zhang, K.; Liao, H.; Ma, Z.; Cheng, F. Effect of curing temperature on the reaction kinetics of cementitious steel slag-fly ash-desulfurized gypsum composites system. *J. Build. Eng.* **2022**, *62*, 105368. [CrossRef]
35. Dutta, R.K.; Khatri, V.N.; Panwar, V. Strength characteristics of fly ash stabilized with lime and modified with phosphogypsum. *J. Build. Eng.* **2017**, *14*, 32–40. [CrossRef]
36. Chen, M.; Liu, P.; Kong, D.; Wang, Y.; Wang, J.; Huang, Y.; Yu, K.; Wu, N. Influencing factors of mechanical and thermal conductivity of foamed phosphogypsum-based composite cementitious materials. *Constr. Build. Mater.* **2022**, *346*, 128462. [CrossRef]
37. Yao, W.; Wu, M.X.; Wei, Y.Q. Determination of reaction degree of silica fume and fly ash in a cement—Silica fume—Fly ash ternary cementitious system. *Chin. J. Mater. Res.* **2014**, *28*, 197–203. (In Chinese)
38. Huo, J.-H.; Peng, Z.-G.; Feng, Q.; Zheng, Y.; Liu, X. Controlling the heat evaluation of cement slurry system used in natural gas hydrate layer by micro-encapsulated phase change materials. *Sol. Energy* **2018**, *169*, 84–93. [CrossRef]
39. Wang, T.; Gao, X.-J.; Wang, J. Preparation of Foamed Phosphogypsum Lightweight Materials by Incorporating Cementitious Additives. *Mater. Sci.-Medzg.* **2019**, *25*, 340–347. [CrossRef]
40. CQuan, Q.; Jiao, C.J.; Yang, Y.Y.; Li, X.B.; Zhang, L. Orthogonal experimental study on mechanical properties of hybrid fiber reinforced concrete. *J. Build. Mater.* **2019**, *22*, 363–370. (In Chinese) [CrossRef]
41. Subasi, A.; Sahin, B.; Kaymaz, I. Multi-objective optimization of a honeycomb heat sink using Response Surface Method. *Int. J. Heat Mass Transf.* **2016**, *101*, 295–302. [CrossRef]